Stabilized high-power laser system for the gravitational wave detector advanced LIGO

P. Kwee,[1,*] C. Bogan,[2] K. Danzmann,[1,2] M. Frede,[4] H. Kim,[1] P. King,[5] J. Pöld,[1] O. Puncken,[3] R. L. Savage,[5] F. Seifert,[5] P. Wessels,[3] L. Winkelmann,[3] and B. Willke[2]

[1]*Max-Planck-Institut für Gravitationsphysik (Albert-Einstein-Institut), Hannover, Germany*
[2]*Leibniz Universität Hannover, Hannover, Germany*
[3]*Laser Zentrum Hannover e.V., Hannover, Germany*
[4]*neoLASE GmbH, Hannover, Germany*
[5]*LIGO Laboratory, California Institute of Technology, Pasadena, California, USA*
**patrick.kwee@aei.mpg.de*

Abstract: An ultra-stable, high-power cw Nd:YAG laser system, developed for the ground-based gravitational wave detector Advanced LIGO (Laser Interferometer Gravitational-Wave Observatory), was comprehensively characterized. Laser power, frequency, beam pointing and beam quality were simultaneously stabilized using different active and passive schemes. The output beam, the performance of the stabilization, and the cross-coupling between different stabilization feedback control loops were characterized and found to fulfill most design requirements. The employed stabilization schemes and the achieved performance are of relevance to many high-precision optical experiments.

OCIS codes: (140.3425) Laser stabilization; (120.3180) Interferometry.

References and links

1. S. Rowan and J. Hough, "Gravitational wave detection by interferometry (ground and space)," Living Rev. Relativity **3**, 1–3 (2000).
2. P. R. Saulson, *Fundamentals of Interferometric Gravitational Wave Detectors* (World Scientific, 1994).
3. G. M. Harry, "Advanced LIGO: the next generation of gravitational wave detectors," Class. Quantum Grav. **27**, 084006 (2010).
4. B. Willke, "Stabilized lasers for advanced gravitational wave detectors," Laser Photon. Rev. **4**, 780–794 (2010).
5. P. Kwee, "Laser characterization and stabilization for precision interferometry," Ph.D. thesis, Universität Hannover (2010).
6. K. Somiya, Y. Chen, S. Kawamura, and N. Mio, "Frequency noise and intensity noise of next-generation gravitational-wave detectors with RF/DC readout schemes," Phys. Rev. D **73**, 122005 (2006).
7. B. Willke, P. King, R. Savage, and P. Fritschel, "Pre-stabilized laser design requirements," internal technical report T050036-v4, LIGO Scientific Collaboration (2009).
8. L. Winkelmann, O. Puncken, R. Kluzik, C. Veltkamp, P. Kwee, J. Poeld, C. Bogan, B. Willke, M. Frede, J. Neumann, P. Wessels, and D. Kracht, "Injection-locked single-frequency laser with an output power of 220 W," Appl. Phys. B **102**, 529–538 (2011).
9. T. J. Kane and R. L. Byer, "Monolithic, unidirectional single-mode Nd:YAG ring laser," Opt. Lett. **10**, 65–67 (1985).
10. I. Freitag, A. Tünnermann, and H. Welling, "Power scaling of diode-pumped monolithic Nd:YAG lasers to output powers of several watts," Opt. Commun. **115**, 511–515 (1995).
11. M. Frede, B. Schulz, R. Wilhelm, P. Kwee, F. Seifert, B. Willke, and D. Kracht, "Fundamental mode, single-frequency laser amplifier for gravitational wave detectors," Opt. Express **15**, 459–465 (2007).

#161737 - $15.00 USD Received 18 Jan 2012; revised 27 Feb 2012; accepted 4 Mar 2012; published 24 Apr 2012

12. A. D. Farinas, E. K. Gustafson, and R. L. Byer, "Frequency and intensity noise in an injection-locked, solid-state laser," J. Opt. Soc. Am. B **12**, 328–334 (1995).
13. R. Bork, M. Aronsson, D. Barker, J. Batch, J. Heefner, A. Ivanov, R. McCarthy, V. Sandberg, and K. Thorne, "New control and data acquisition system in the Advanced LIGO project," Proc. of Industrial Control And Large Experimental Physics Control System (ICALEPSC) conference (2011).
14. "Experimental physics and industrial control system," `http://www.aps.anl.gov/epics/`.
15. P. Kwee and B. Willke, "Automatic laser beam characterization of monolithic Nd:YAG nonplanar ring lasers," Appl. Opt. **47**, 6022–6032 (2008).
16. P. Kwee, F. Seifert, B. Willke, and K. Danzmann, "Laser beam quality and pointing measurement with an optical resonator," Rev. Sci. Instrum. **78**, 073103 (2007).
17. A. Rüdiger, R. Schilling, L. Schnupp, W. Winkler, H. Billing, and K. Maischberger, "A mode selector to suppress fluctuations in laser beam geometry," Opt. Acta **28**, 641–658 (1981).
18. B. Willke, N. Uehara, E. K. Gustafson, R. L. Byer, P. J. King, S. U. Seel, and R. L. Savage, "Spatial and temporal filtering of a 10-W Nd:YAG laser with a Fabry-Perot ring-cavity premode cleaner," Opt. Lett. **23**, 1704–1706 (1998).
19. J. H. Pöld, "Stabilization of the Advanced LIGO 200 W laser," Diploma thesis, Leibniz Universität Hannover (2009).
20. E. D. Black, "An introduction to Pound-Drever-Hall laser frequency stabilization," Am. J. Phys. **69**, 79–87 (2001).
21. R. W. P. Drever, J. L. Hall, F. V. Kowalski, J. Hough, G. M. Ford, A. J. Munley, and H. Ward, "Laser phase and frequency stabilization using an optical resonator," Appl. Phys. B **31**, 97–105 (1983).
22. A. Bullington, B. Lantz, M. Fejer, and R. Byer, "Modal frequency degeneracy in thermally loaded optical resonators," Appl. Opt. **47**, 2840–2851 (2008).
23. G. Mueller, "Beam jitter coupling in Advanced LIGO," Opt. Express **13**, 7118–7132 (2005).
24. V. Delaubert, N. Treps, M. Lassen, C. C. Harb, C. Fabre, P. K. Lam, and H.-A. Bachor, "TEM_{10} homodyne detection as an optimal small-displacement and tilt-measurement scheme," Phys. Rev. A **74**, 053823 (2006).
25. P. Kwee, B. Willke, and K. Danzmann, "Laser power noise detection at the quantum-noise limit of 32 A photocurrent," Opt. Lett. **36**, 3563–3565 (2011).
26. A. Araya, N. Mio, K. Tsubono, K. Suehiro, S. Telada, M. Ohashi, and M. Fujimoto, "Optical mode cleaner with suspended mirrors," Appl. Opt. **36**, 1446–1453 (1997).
27. P. Kwee, B. Willke, and K. Danzmann, "Shot-noise-limited laser power stabilization with a high-power photodiode array," Opt. Lett. **34**, 2912–2914 (2009).
28. B. Lantz, P. Fritschel, H. Rong, E. Daw, and G. González, "Quantum-limited optical phase detection at the 10^{-10} rad level," J. Opt. Soc. Am. A **19**, 91–100 (2002).

1. Introduction

Interferometric gravitational wave detectors [1, 2] perform one of the most precise differential length measurements ever. Their goal is to directly detect the faint signals of gravitational waves emitted by astrophysical sources. The Advanced LIGO (Laser Interferometer Gravitational-Wave Observatory) [3] project is currently installing three second-generation, ground-based detectors at two observatory sites in the USA. The 4 kilometer-long baseline Michelson interferometers have an anticipated tenfold better sensitivity than their first-generation counterparts (Inital LIGO) and will presumably reach a strain sensitivity between 10^{-24} and $10^{-23}\,\mathrm{Hz}^{-1/2}$.

One key technology necessary to reach this extreme sensitivity are ultra-stable high-power laser systems [4, 5]. A high laser output power is required to reach a high signal-to-quantum-noise ratio, since the effect of quantum noise at high frequencies in the gravitational wave readout is reduced with increasing circulating laser power in the interferometer. In addition to quantum noise, technical laser noise coupling to the gravitational wave channel is a major noise source [6]. Thus it is important to reduce the coupling of laser noise, e.g. by optical design or by exploiting symmetries, and to reduce laser noise itself by various active and passive stabilization schemes.

In this article, we report on the pre-stabilized laser (PSL) of the Advanced LIGO detector. The PSL is based on a high-power solid-state laser that is comprehensively stabilized. One laser system was set up at the Albert-Einstein-Institute (AEI) in Hannover, Germany, the so called PSL reference system. Another identical PSL has already been installed at one Advanced LIGO site, the one near Livingston, LA, USA, and two more PSLs will be installed at the second

#161737 - $15.00 USD Received 18 Jan 2012; revised 27 Feb 2012; accepted 4 Mar 2012; published 24 Apr 2012

site at Hanford, WA, USA. We have characterized the reference PSL and the first observatory PSL. For this we measured various beam parameters and noise levels of the output beam in the gravitational wave detection frequency band from about 10 Hz to 10 kHz, measured the performance of the active and passive stabilization schemes, and determined upper bounds for the cross coupling between different control loops.

At the time of writing the PSL reference system has been operated continuously for more than 18 months, and continues to operate reliably. The reference system delivered a continuous-wave, single-frequency laser beam at 1064 nm wavelength with a maximum power of 150 W with 99.5% in the TEM_{00} mode. The active and passive stabilization schemes efficiently reduced the technical laser noise by several orders of magnitude such that most design requirements [5, 7] were fulfilled. In the gravitational wave detection frequency band the relative power noise was as low as $2 \times 10^{-8}\,\mathrm{Hz}^{-1/2}$, relative beam pointing fluctuations were as low as $1 \times 10^{-7}\,\mathrm{Hz}^{-1/2}$, and an in-loop measurement of the frequency noise was consistent with the maximum acceptable frequency noise of about $0.1\,\mathrm{Hz}\,\mathrm{Hz}^{-1/2}$. The cross couplings between the control loops were, in general, rather small or at the expected levels. Thus we were able to optimize each loop individually and observed no instabilities due to cross couplings.

This stabilized laser system is an indispensable part of Advanced LIGO and fulfilled nearly all design goals concerning the maximum acceptable noise levels of the different beam parameters right after installation. Furthermore all or a subset of the implemented stabilization schemes might be of interest for many other high-precision optical experiments that are limited by laser noise. Besides gravitational wave detectors, stabilized laser systems are used e.g. in the field of optical frequency standards, macroscopic quantum objects, precision spectroscopy and optical traps.

In the following section the laser system, the stabilization scheme and the characterization methods are described (Section 2). Then, the results of the characterization (Section 3) and the conclusions (Section 4) are presented.

2. Laser system and stabilization

The PSL consists of the laser, developed and fabricated by Laser Zentrum Hannover e.V. (LZH) and neoLASE, and the stabilization, developed and integrated by AEI.

The optical components of the PSL are on a commercial optical table, occupying a space of about $1.5 \times 3.5\,\mathrm{m}^2$, in a clean, dust-free environment. At the observatory sites the optical table is located in an acoustically isolated cleanroom. Most of the required electronics, the laser diodes for pumping the laser, and water chillers for cooling components on the optical table are placed outside of this cleanroom.

The laser itself consists of three stages (Fig. 1). An almost final version of the laser, the so-called engineering prototype, is described in detail in [8]. The primary focus of this article is the stabilization and characterization of the PSL. Thus only a rough overview of the laser and the minor modifications implemented between engineering prototype and reference system are given in the following.

The first stage, the master laser, is a commercial non-planar ring-oscillator [9, 10] (NPRO) manufactured by InnoLight GmbH in Hannover, Germany. This solid-state laser uses a Nd:YAG crystal as the laser medium and resonator at the same time. The NPRO is pumped by laser diodes at 808 nm and delivers an output power of 2 W. An internal power stabilization, called the noise eater, suppresses the relaxation oscillation at around 1 MHz. Due to its monolithic resonator, the laser has exceptional intrinsic frequency stability. The two subsequent laser stages, used for power scaling, inherit the frequency stability of the master laser.

The second stage (medium-power amplifier) is a single-pass amplifier [11] with an output power of 35 W. The seed laser beam from the NPRO stage passes through four Nd:YVO_4 crys-

#161737 - $15.00 USD Received 18 Jan 2012; revised 27 Feb 2012; accepted 4 Mar 2012; published 24 Apr 2012

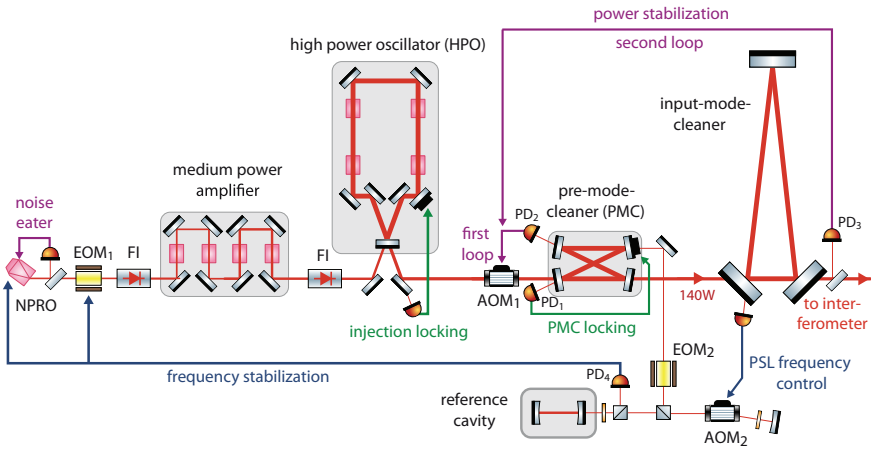

Fig. 1. Pre-stabilized laser system of Advanced LIGO. The three-staged laser (NPRO, medium power amplifier, high power oscillator) and the stabilization scheme (pre-mode-cleaner, power and frequency stabilization) are shown. The input-mode-cleaner is not part of the PSL but closely related. NPRO, non-planar ring oscillator; EOM, electro-optic modulator; FI, Faraday isolator; AOM, acousto-optic modulator.

tals which are longitudinally pumped by fiber-coupled laser diodes at 808 nm.

The third stage is an injection-locked ring oscillator [8] with an output power of about 220 W, called the high-power oscillator (HPO). Four Nd:YAG crystals are used as the active media. Each is longitudinally pumped by seven fiber-coupled laser diodes at 808 nm. The oscillator is injection-locked [12] to the previous laser stage using a feedback control loop. A broadband EOM (electro-optic modulator) placed between the NPRO and the medium-power amplifier is used to generate the required phase modulation sidebands at 35.5 MHz. Thus the high output power and good beam quality of this last stage is combined with the good frequency stability of the previous stages.

The reference system features some minor modifications compared to the engineering prototype [8] concerning the optics: The external halo aperture was integrated into the laser system permanently improving the beam quality. Additionally, a few minor design flaws related to the mechanical structure and the optical layout were engineered out. This did not degrade the output performance, nor the characteristics of the locked laser.

In general the PSL is designed to be operated in two different power modes. In high-power mode all three laser stages are engaged with a power of about 160 W at the PSL output. In low-power mode the high-power oscillator is turned off and a shutter inside the laser resonator is closed. The beam of the medium-power stage is reflected at the output coupler of the high power stage leaving a residual power of about 13 W at the PSL output. This low-power mode will be used in the early commissioning phase and in the low-frequency-optimized operation mode of Advanced LIGO and is not discussed further in this article.

The stabilization has three sections (Fig. 1: PMC, PD_2, reference cavity): A passive resonator, the so called pre-mode-cleaner (PMC), is used to filter the laser beam spatially and temporally (see subsection 2.1). Two pick-off beams at the PMC are used for the active power stabilization (see subsection 2.2) and the active frequency pre-stabilization, respectively (see subsection 2.3).

In general most stabilization feedback control loops of the PSL are implemented using analog electronics. A real-time computer system (Control and Data Acquisition Systems, CDS, [13]) which is common to many other subsystems of Advanced LIGO, is utilized to control and monitor important parameters of the analog electronics. The lock acquisition of various loops, a few

#161737 - $15.00 USD Received 18 Jan 2012; revised 27 Feb 2012; accepted 4 Mar 2012; published 24 Apr 2012

slow digital control loops, and the data acquisition are implemented using this computer system. Many signals are recorded at different sampling rates ranging from 16 Hz to 33 kHz for diagnostics, monitoring and vetoing of gravitational wave signals. In total four real-time processes are used to control different aspects of the laser system. The Experimental Physics and Industrial Control System (EPICS) [14] and its associated user tools are used to communicate with the real-time software modules.

The PSL contains a permanent, dedicated diagnostic instrument, the so called diagnostic breadboard (DBB, not shown in Fig. 1) [15]. This instrument is used to analyze two different beams, pick-off beams of the medium power stage and of the HPO. Two shutters are used to multiplex these to the DBB. We are able to measure fluctuations in power, frequency and beam pointing in an automated way with this instrument. In addition the beam quality quantified by the higher order mode content of the beam was measured using a modescan technique [16]. The DBB is controlled by one real-time process of the CDS. In contrast to most of the other control loops in the PSL, all DBB control loops were implemented digitally. We used this instrument during the characterization of the laser system to measure the mentioned laser beam parameters of the HPO. In addition we temporarily placed an identical copy of the DBB downstream of the PMC to characterize the output beam of the PSL reference system.

2.1. Pre-mode-cleaner

A key component of the stabilization scheme is the passive ring resonator, called the pre-mode-cleaner (PMC) [17, 18]. It functions to suppress higher-order transverse modes, to improve the beam quality and the pointing stability of the laser beam, and to filter power fluctuations at radio frequencies. The beam transmitted through this resonator is the output beam of the PSL, and it is delivered to the subsequent subsystems of the gravitational wave detector.

We developed and used a computer program [19] to model the filter effects of the PMC as a function of various resonator parameters in order to aid its design. This led to a resonator with a bow-tie configuration consisting of four low-loss mirrors glued to an aluminum spacer. The optical round-trip length is 2 m with a free spectral range (FSR) of 150 MHz. The incidence angle of the horizontally polarized laser beam is 6°. The flat input and output coupling mirrors have a power transmission of 2.4% and the two concave high reflectivity mirrors (3 m radius of curvature) have a transmission of 68 ppm. The measured bandwidth was, as expected, 560 kHz which corresponds to a finesse of 133 and a power build-up factor of 42. The Gaussian input/output beam had a waist radius of about 568 μm and the measured acquired round-trip Gouy phase was about 1.7 rad which is equivalent to 0.27 FSR.

One TEM_{00} resonance frequency of the PMC is stabilized to the laser frequency. The Pound-Drever-Hall (PDH) [20, 21] sensing scheme is used to generate error signals, reusing the phase modulation sidebands at 35.5 MHz created between NPRO and medium power amplifier for the injection locking. The signal of the photodetector PD_1, placed in reflection of the PMC, is demodulated at 35.5 MHz. This photodetector consists of a 1 mm InGaAs photodiode and a transimpedance amplifier. A piezo-electric element (PZT) between one of the curved mirrors and the spacer is used as a fast actuator to control the round-trip length and thereby the resonance frequencies of the PMC. With a maximum voltage of 382 V we were able to change the round-trip length by about 2.4 μm. An analog feedback control loop with a bandwidth of about 7 kHz is used to stabilize the PMC resonance frequency to the laser frequency.

In addition, the electronics is able to automatically bring the PMC into resonance with the laser (lock acquisition). For this process a 125 ms period ramp signal with an amplitude corresponding to about one FSR is applied to the PZT of the PMC. The average power on photodetector PD_1 is monitored and as soon as the power drops below a given threshold the logic considers the PMC as resonant and closes the analog control loop. This lock acquisition proce-

#161737 - $15.00 USD Received 18 Jan 2012; revised 27 Feb 2012; accepted 4 Mar 2012; published 24 Apr 2012

dure took an average of about 65 ms and is automatically repeated as soon as the PMC goes off resonance.

One real-time process of CDS is dedicated to control the PMC electronics. This includes parameters such as the proportional gain of the loop or lock acquisition parameters. In addition to the PZT actuator, two heating foils, delivering a maximum total heating power of 14 W, are attached to the aluminum spacer to control its temperature and thereby the roundtrip length on timescales longer than 3 s. We measured a heating and cooling $1/e$ time constant of about 2 h with a range of 4.5 K which corresponds to about 197 FSR. During maintenance periods we heat the spacer with 7 W to reach a spacer temperature of about 2.3 K above room temperature in order to optimize the dynamic range of this actuator. A digital control loop uses this heater as an actuator to off-load the PZT actuator allowing compensation for slow room temperature and laser frequency drifts.

The PMC is placed inside a pressure-tight tank at atmospheric pressure for acoustic shielding, to avoid contamination of the resonator mirrors and to minimize optical path length changes induced by atmospheric pressure variations. We used only low-outgassing materials and fabricated the PMC in a cleanroom in order to keep the initial mirror contamination to a minimum and to sustain a high long-term throughput.

The PMC filters the laser beam and improves the beam quality of the laser by suppressing higher order transverse modes [17]. The acquired round-trip Gouy phase of the PMC was chosen in such a way that the resonance frequencies of higher order TEM modes are clearly separated from the TEM_{00} resonance frequency. Thus these modes are not resonant and are mainly reflected by the PMC, whereas the TEM_{00} mode is transmitted. However, during the design phase we underestimated the thermal effects in the PMC such that at nominal circulating power the round-trip Gouy-phase is close to 0.25 FSR and the resonance of the TEM_{40} mode is close to that of the TEM_{00} mode. To characterize the mode-cleaning performance we measured the beam quality upstream and downstream of the PMC with the two independent DBBs.

At 150 W in the transmitted beam, the circulating power in the PMC is about 6.4 kW and the intensity at the mirror surface can be as high as $1.8 \times 10^{10}\,\mathrm{W\,m^{-2}}$. At these power levels even small absorptions in the mirror coatings cause thermal effects which slightly change the mirror curvature [22]. To estimate these thermal effects we analyzed the transmitted beam as a function of the circulating power using the DBB. In particular we measured the mode content of the LG_{10} and TEM_{40} mode. Changes of the PMC eigenmode waist size showed up as variations of the LG_{10} mode content. A power dependence of the round-trip Gouy phase caused a variation of the power within the TEM_{40} mode since its resonance frequency is close to a TEM_{00} mode resonance and thus the suppression of this mode depends strongly on the Gouy phase. We adjusted the input power to the PMC such that the transmitted power ranged from 100 W to 150 W corresponding to a circulating power between 4.2 kW and 6.4 kW. We used our PMC computer simulation to deduce the power dependence of the eigenmode waist size and the round-trip Gouy phase. The results are given in section 3.1.

At all circulating power levels, however, the TEM_{10} and TEM_{01} modes are strongly suppressed by the PMC and thus beam pointing fluctuations are reduced. Pointing fluctuations can be expressed to first order as power fluctuations of the TEM_{10} and TEM_{01} modes [23, 24]. The PMC reduces the field amplitude of these modes and thus the pointing fluctuations by a factor of about 61 according to the measured finesse and round-trip Gouy phase. To keep beam pointing fluctuations small is important since they couple to the gravitational wave channel by small differential misalignments of the interferometer optics. Thus stringent design requirements, at the $10^{-6}\,\mathrm{Hz}^{-1/2}$ level for relative pointing, were set. To verify the pointing suppression effect of the PMC we used DBBs to measure the beam pointing fluctuations upstream and downstream

#161737 - $15.00 USD Received 18 Jan 2012; revised 27 Feb 2012; accepted 4 Mar 2012; published 24 Apr 2012

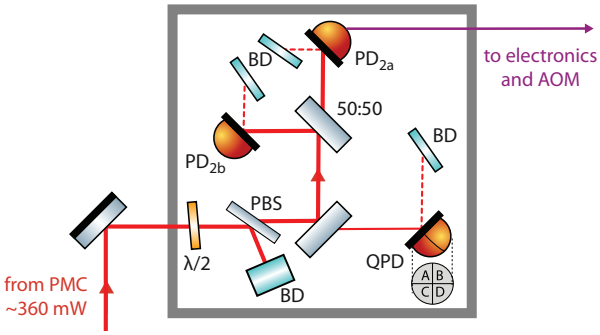

Fig. 2. Detailed schematic of the power noise sensor setup for the first power stabilization loop. This setup corresponds to PD_2 in the overview in Fig. 1. $\lambda/2$, waveplate; PBS, polarizing beam splitter; BD, glass filters used as beam dump; PD, single element photodetector; QPD, quadrant photodetector.

of the PMC.

The resonator design has an even number of nearly normal-incidence reflections. Thus the resonance frequencies of horizontal and vertical polarized light are almost identical and the PMC does not act as polarizer. Therefore we use a thin-film polarizer upstream of the PMC to reach the required purity of larger than 100:1 in horizontal polarization.

Finally the PMC reduces technical power fluctuations at radio frequencies (RF). A good power stability between 9 MHz and 100 MHz is necessary as the phase modulated light injected into the interferometer is used to sense several degrees of freedom of the interferometer that need to be controlled. Power noise around these phase modulation sidebands would be a noise source for the respective stabilization loop. The PMC has a bandwidth (HWHM) of about 560 kHz and acts to first order as a low-pass filter for power fluctuations with a -3 dB corner frequency at this frequency. To verify that the suppression of RF power fluctuations is sufficient to fulfill the design requirements, we measured the relative power noise up to 100 MHz downstream of the PMC with a dedicated experiment involving the optical ac coupling technique [25].

In addition the PMC serves the very important purpose of defining the spatial laser mode for the downstream subsystem, namely the input optics (IO) subsystem. The IO subsystem is responsible, among other things, to further stabilize the laser beam with the suspended input mode cleaner [26] before the beam will be injected into the interferometer. Modifications of beam alignment or beam size of the laser system, which were and might be unavoidable, e.g., due to maintenance, do not propagate downstream of the PMC to first order due to its mode-cleaning effect. Furthermore we benefit from a similar isolating effect for the active power and frequency stabilization by using the beams transmitted through the curved high-reflectivity mirrors of the PMC.

2.2. Power stabilization

The passive filtering effect of the PMC reduces power fluctuations significantly only above the PMC bandwidth. In the detection band from about 10 Hz to 10 kHz good power stability is required since fluctuations couple via the radiation pressure imbalance and the dark-fringe offset to the gravitational wave channel. Thus two cascaded active control loops, the first and second power stabilization loop, are used to reduce power fluctuations which are mainly caused by the HPO stage.

The first loop uses a low-noise photodetector (PD_2, see Figs. 1 and 2) at one pick-off port

#161737 - $15.00 USD Received 18 Jan 2012; revised 27 Feb 2012; accepted 4 Mar 2012; published 24 Apr 2012

of the PMC to measure the power fluctuations downstream of the PMC. An analog electronics feedback control loop and an AOM (acousto-optic modulator) as actuator, located upstream of the PMC, are used to stabilize the power.

Scattered light turned out to be a critical noise source for this first loop. Thus we placed all required optical and opto-electronic components into a box to shield from scattered light (see Fig. 2). The beam transmitted by the curved PMC mirror has a power of about 360 mW. This beam is first attenuated in the box using a $\lambda/2$ waveplate and a thin-film polarizer, such that we are able to adjust the power on the photodetectors to the optimal operation point. Afterwards the beam is split by a 50:50 beam splitter. The beams are directed to two identical photodetectors, one for the control loop (PD_{2a}, in-loop detector) and one for independent out-of-loop measurements to verify the achieved power stability (PD_{2b}, out-of-loop detector). These photodetectors consist of a 2 mm InGaAs photodiode (PerkinElmer C30642GH), a transimpedance amplifier and an integrated signal-conditioning filter. At the chosen operation point a power of about 4 mW illuminates each photodetector generating a photocurrent of about 3 mA. Thus the shot noise is at a relative power noise of $10^{-8}\,\mathrm{Hz}^{-1/2}$. The signal conditioning filter has a gain of 0.2 at very low frequencies (< 70 mHz) and amplifies the photodetector signal in the important frequency range between 3.3 Hz and 120 Hz by about 52 dB. This signal conditioning filter reduces the electronics noise requirements on all subsequent stages, but has the drawback that the range between 3.3 Hz and 120 Hz is limited to maximum peak-to-peak relative power fluctuations of 5×10^{-3}. Thus the signal-conditioned channel is in its designed operation range only when the power stabilization loop is closed and therefore it is not possible to measure the free running power noise using this channel due to saturation.

The uncoated glass windows of the photodiodes were removed and the laser beam hits the photodiodes at an incidence angle of 45°. The residual reflection from the photodiode surface is dumped into a glass filter (Schott BG39) at the Brewster angle.

Beam position fluctuations in combination with spatial inhomogeneities in the photodiode responsivity is another noise source for the power stabilization. We placed a silicon quadrant photodetector (QPD) in the box to measure the beam position fluctuations of a low-power beam picked off the main beam in the box. The beam parameters, in particular the Gouy phase, at the QPD are the same as on the power sensing detectors. Thus the beam position fluctuations measured with the QPD are the same as the ones on the power sensing photodetectors, assuming that the position fluctuations are caused upstream of the QPD pick-off point. We used the QPD to measure beam position fluctuations only for diagnostic and noise projection purposes.

In a slightly modified experiment, we replaced one turning mirror in the path to the power stabilization box by a mirror attached to a tip/tilt PZT element. We measured the typical coupling between beam position fluctuations generated by the PZT and the residual relative photocurrent fluctuations measured with the out-of-the-loop photodetector. This coupling was between $1\,\mathrm{m}^{-1}$ and $10\,\mathrm{m}^{-1}$ which is a typical value observed in different power stabilization experiments as well. We measured this coupling factor to be able to calculate the noise contribution in the out-of-the-loop photodetector signal due to beam position fluctuations (see Subsection 3.3). Since this tip/tilt actuator was only temporarily in the setup, we are not able to measure the coupling on a regular basis.

Both power sensing photodetectors are connected to analog feedback control electronics. A low-pass (100 mHz corner frequency) filtered reference value is subtracted from one signal which is subsequently passed through several control loop filter stages. With power stabilization activated, we are able to control the power on the photodetectors and thereby the PSL output power via the reference level on time scales longer than 10 s. The reference level and other important parameters of these electronics are controlled by one dedicated real-time process of the CDS. The actuation or control signal of the electronics is passed to an AOM driver

#161737 - $15.00 USD Received 18 Jan 2012; revised 27 Feb 2012; accepted 4 Mar 2012; published 24 Apr 2012

controlling the output amplitude of its 80 MHz signal. The AOM driver (Neos 21080-2AM-RFX) has a maximum output power of 2 W and is connected to the AOM (Crystal Technologies, 3080-199). This AOM is placed between the HPO and the PMC. The zeroth order beam is directed to the PMC, whereas the first diffraction order is dumped. Thus we are able to control the beam power directed to the PMC. The small-signal transfer function from the input signal of the AOM driver to a power modulation downstream of the AOM is flat up to about 200 kHz. At 120 kHz we measured a phase lag of 45°. We fitted a time delay to the measured transfer function yielding a delay of about 1 μs.

The power diffracted by the AOM is a quadratic function of the amplitude of the 80 MHz drive signal. Thus, depending on the operation point, the equivalent proportional gain of the actuator in the control loop changes, which alters the loop gain and in the worst case the stability of this control loop. To prevent such effects the electronics contains an analog multiplier integrated circuit (IC), used to determine the square root of the control signal to compensate the quadratic function.

The dc-coupled control loop has a unity gain frequency of 60 kHz with more than 20 dB loop gain for frequencies below 10 kHz. The loop gain is sufficient to suppress the power fluctuations below the design requirement level.

In general this control loop does not require a start-up procedure equivalent to the lock-acquisition of the PMC control loop because a valid error signal is always present. However, since the photodetector internal signal conditioning filter is, in general, saturated due to the high free-running power fluctuations of the laser, it takes a couple of seconds until the filter settles. During this time it often occurred that more power than necessary was diffracted, influencing other control loops in the worst case. We implemented a digital start-up procedure using the CDS to reduce these transient oscillations. During start-up we use the photodetector signal upstream of the signal conditioning filter to first stabilize the laser power with a low-bandwidth digital loop. Due to the missing signal conditioning filter this loop is not able reach the required noise performance but reduces the power fluctuations to a level such that the signal conditioning filters were able to settle. After a few seconds this digital control loop is turned off and the analog low-noise, high-bandwidth first power stabilization loop is closed.

The primary task of the first power stabilization loop is to reduce the relative power fluctuations by about three orders of magnitude to the goal of $2 \times 10^{-8}\,\mathrm{Hz}^{-1/2}$ and therefore reducing the loop-gain required for the second power stabilization loop which is responsible for the ultimate power stability in the interferometer. To verify the achieved performance we measured the relative power fluctuations with a second power sensing photodetector, the out-of-loop detector, which is connected via the electronics to the CDS system for data acquisition.

The second power stabilization loop with a photodetector (PD_3) directly upstream of the interferometer is used to reach the required power stability of $2 \times 10^{-9}\,\mathrm{Hz}^{-1/2}$ at 10 Hz at the input of the interferometer. The first-loop power stability is further improved and expected power noise introduced between the PMC and the input of the interferometer noise will be compensated. This stabilization is being developed at the moment, so the design has not been finalized. Since the acceptable residual relative power noise is one order of magnitude below the goal of the first loop, a different high-power, low-noise photodetector is necessary which will detect a laser power of > 100 mW. An array of photodiodes located on a seismically isolated platform in an ultra high vacuum tank (Advanced LIGO vacuum chamber) will be used. Depending on the level of power fluctuations at this location a slower, more flexible digital or a faster analog second power stabilization loop will be realized. In any case the control or actuation signal of the second loop will be injected into the error point of the first loop. Thus the first loop acts as power actuator for the second loop. The signal conditioning filters in the photodetectors of the first loop limits the range of this power actuator. Hence a maximum peak-to-peak relative

#161737 - $15.00 USD Received 18 Jan 2012; revised 27 Feb 2012; accepted 4 Mar 2012; published 24 Apr 2012

power of 5×10^{-3} can be actuated using the first loop. This sets requirements on the maximum power fluctuation introduced between the PMC and the input of the interferometer. In a precursor experiment [27] we demonstrated that it is possible to build a photodetector with the required sensitivity of $2 \times 10^{-9}\,\mathrm{Hz}^{-1/2}$.

2.3. Frequency stabilization

Good frequency stability is required for lock acquisition of the interferometer and to reduce the frequency noise coupling into the gravitational wave channel via asymmetries in the interferometer arms. The frequency stabilization of the PSL is only a pre-stabilization to an optical reference cavity located on the laser table. The final stabilization for the gravitational wave detector will be reached by stabilizing the laser frequency to a frequency reference set by the long-baseline arm cavities of the interferometer.

The acceptable frequency noise of the PSL is about three orders of magnitude below the free running frequency noise of the laser, which is dominated by the NPRO laser. Thus active stabilization is necessary. The stabilization concept is very similar to the frequency stabilization of the Initial LIGO detector [28]: A linear rigid-spacer reference cavity, the PDH sensing scheme, and a compound actuator consisting of NPRO actuators and a broad-band phase-shifting EOM are used.

The reference cavity consists of a 203 mm long fused silica spacer with optically contacted low-loss, high-reflectivity mirrors. Both concave mirrors have a radius of curvature of 0.5 m. The cavity is suspended by an eddy current damped single pendulum stage which is supported by a passive vibration isolation stack in ultra-high vacuum (UHV). A pressure below 10^{-6} Pa is reached using an ion getter pump. In this way the resonator is isolated from external noise sources in order to achieve good length stability and with it high frequency stability. The reference cavity, the vibration isolation, and the vacuum tank are reused from Initial LIGO. The cavity has a FSR of 737 MHz and we measured a bandwidth (HWHM) of 32 kHz which corresponds to a finesse of 11 500. We observed that TEM modes of equal order were not fully degenerate, as we expected for this linear resonator. Thus the Gouy phase seemed to be slightly different in the horizontal and vertical directions. This frequency splitting is not an issue for the frequency pre-stabilization of Advanced LIGO since the TEM_{00} mode that is the only one of zeroth order is used for the stabilization.

The vacuum tank is temperature stabilized with attached heaters to a few Kelvin above room temperature. Several temperature sensors at the vacuum tank are used as control loop sensors. In addition the tank is thermally isolated with an enclosure. This temperature stabilization is required since the room temperature fluctuations (less than ± 2 K) in combination with the thermal expansion of fused silica are too large to fulfill the long-term frequency stability design requirements. The temperature dependence of the resonator's resonance frequency, 155 MHz/K, requires a temperature stability of better than 5 mK.

The laser frequency is stabilized to one TEM_{00} mode resonance of the reference cavity. For this the beam from the pick-off at the PMC is passed through a resonant EOM (EOM_2) to create phase modulation sidebands at 21.5 MHz with a modulation index of 0.6 rad. These sidebands are necessary for the PDH [20, 21] frequency stabilization scheme. Afterwards the laser beam frequency is shifted by an AOM (AOM_2) in a double-pass configuration by twice the RF driver frequency. This AOM is used as actuator for the PSL frequency by other interferometer subsystems, as described in more detail later in this subsection. We achieved a double pass efficiency of only 15% which needs to be optimized in the future to reach the required power levels at and downstream of the reference cavity. The frequency shifted beam, which has a power of about 33 mW, is directed to the reference cavity. The retro-reflected beam is separated via polarizing optics from the incoming beam and is directed to a resonant photodetector (PD_4). This pho-

#161737 - $15.00 USD Received 18 Jan 2012; revised 27 Feb 2012; accepted 4 Mar 2012; published 24 Apr 2012

todetector consists of a 2 mm InGaAs photodiode (PerkinElmer C30642GH) and a resonance circuit tuned to 21.5 MHz. A photocurrent of 7.8 mA, off resonance, and of 4.2 mA, on resonance, were detected. The photodetector signal is passed to the control loop electronics module which is located on the optical table to reduce the cable length and thereby time delays and phase lags. In these electronics the signal is demodulated to generate the PDH error signals and is passed to the filters for the feedback control loop. A compound actuator is used to stabilize the laser frequency. The actuator consists of a PZT, attached to the NPRO crystal, and the broadband EOM (EOM_1) used as phase corrector between NPRO and medium power amplifier. The cross-over frequency between these two actuators is about 10 kHz. For lower frequencies the PZT, and for higher frequencies the EOM, is used as the frequency actuator.

One real-time process is dedicated to controlling the frequency stabilization. Most parameters of the analog electronics and the feedback control loop are set via the CDS. For timescales of the order of 1 s and longer a digital control loop actuating on the NPRO crystal temperature is used to control the laser frequency and to off-load the PZT actuator. By using these three different frequency actuators a high unity-gain frequency of about 330 kHz, on the one hand, and a high range of several gigahertz on long time scales, on the other hand, are achieved. This high unity-gain frequency is necessary to achieve the required loop gain of more than 20 dB below 100 kHz. The loop-gain design requirement is derived from the required bandwidth for controlling the PSL frequency via the frequency-shifting AOM, as described later on in this subsection.

The lock acquisition is performed automatically by the CDS in several stages. During the first stage the NPRO crystal temperature is slowly ramped while an additional 10 Hz ramp with an amplitude of about 500 cavity linewidths is applied to the NPRO PZT. A photodetector in transmission of the reference cavity is used to detect if the laser frequency swept over a resonance of the reference cavity. In that case an intermediate digital control loop is closed, trying to center the resonance peak on the 10 Hz ramp by actuating on the NPRO temperature. During the next stage the 10 Hz ramp is turned off and the analog control loop is closed, slowly ramping the proportional gain up to the final value. During the final stage a digital temperature control loop is closed to off-load the PZT actuator by actuating on the NPRO temperature. The CDS monitors the power on the photodetector in transmission of the reference cavity and as soon as the power drops below a given threshold, the reference cavity is considered non-resonant and the lock acquisition procedure is repeated. The average lock acquisition duration is shorter than 50 s from a cold start.

The Interferometer Sensing and Control (ISC) subsystem of the gravitational wave detector needs to be able to control the PSL laser frequency in order to keep the gravitational wave detector at the desired operation point. Since the resonance frequency of the reference cavity can be changed only very slowly via its temperature, the frequency shifting AOM is introduced between the PMC pick-off and the reference cavity. The drive frequency of the AOM is around 80 MHz and is generated by a voltage control oscillator (VCO). With this setup we are able to shift the laser frequency within a range of about 14 MHz (152 . . . 166 MHz) peak-to-peak with a measured actuation bandwidth of 10 kHz using the VCO. However, the interferometer control concept of Advanced LIGO needs a higher bandwidth of 50 kHz. Thus this aspect of the frequency stabilizations needs further optimization in the future and we suspect that the delay due to the acoustic wave in the AOM is the main bandwidth limitation.

An alternative control input would be the error point of the frequency stabilization control loop. By adding a signal to the error point the control loop will adjust the laser frequency to compensate the added signal. Using this control input we achieve a range of several kilohertz and a bandwidth of more than 100 kHz. The advantage of this control input is its higher bandwidth. However, it has a smaller range and a higher cross-coupling between power noise and

#161737 - $15.00 USD Received 18 Jan 2012; revised 27 Feb 2012; accepted 4 Mar 2012; published 24 Apr 2012

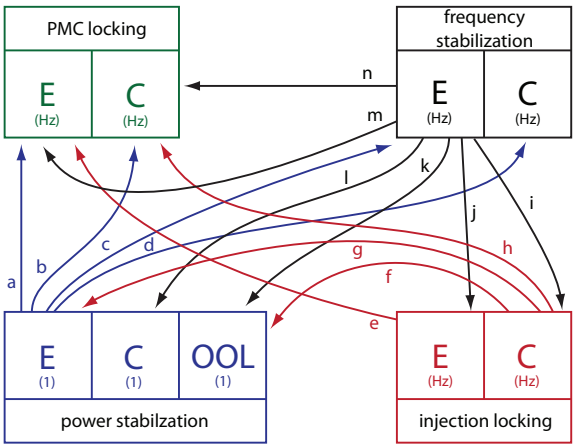

	Magnitude	Frequency band
a	$< 10^{6}\,\mathrm{Hz}/1$	$10\,\mathrm{Hz}\ldots100\,\mathrm{kHz}$
b	$< 10^{8}\,\mathrm{Hz}/1$	$10\,\mathrm{Hz}\ldots100\,\mathrm{kHz}$
c	$< 10^{2}\ldots10^{3}\,\mathrm{Hz}/1$	$10\,\mathrm{Hz}\ldots100\,\mathrm{kHz}$
d	$< 10^{8}\,\mathrm{Hz}/1$	$10\,\mathrm{Hz}\ldots100\,\mathrm{kHz}$
e	$\approx 0.1\,\mathrm{Hz}/\mathrm{Hz}$	$10\,\mathrm{Hz}\ldots10\,\mathrm{kHz}$
f	$< 10^{-12}\,1/\mathrm{Hz}$	$10\,\mathrm{Hz}\ldots1\,\mathrm{kHz}$
g	$< 10^{-12}\,1/\mathrm{Hz}$	$10\,\mathrm{Hz}\ldots1\,\mathrm{kHz}$
h	$\approx 5\times10^{-2}\,\mathrm{Hz}/\mathrm{Hz}$	$10\,\mathrm{Hz}\ldots10\,\mathrm{kHz}$
i	$\approx 10^{3}\,\mathrm{Hz}/\mathrm{Hz}$	$10\,\mathrm{Hz}\ldots1\,\mathrm{kHz}$
j	$\approx 0.1\ldots10\,\mathrm{Hz}/\mathrm{Hz}$	$10\,\mathrm{Hz}\ldots100\,\mathrm{kHz}$
k	$< 10^{-9}\,1/\mathrm{Hz}$	$10\,\mathrm{Hz}\ldots1\,\mathrm{kHz}$
l	$< 10^{-6}\,1/\mathrm{Hz}$	$10\,\mathrm{Hz}\ldots100\,\mathrm{kHz}$
m	$\approx 10^{-3}\ldots10^{-2}\,\mathrm{Hz}/\mathrm{Hz}$	$10\,\mathrm{Hz}\ldots1\,\mathrm{kHz}$
n	$\approx 1\,\mathrm{Hz}/\mathrm{Hz}$	$10\,\mathrm{Hz}\ldots10\,\mathrm{kHz}$

Fig. 3. Cross coupling transfer functions (a…n) were measured between four different control loops. Measurements between the error signal (E), the control signal (C), and in the case of the power stabilization loop the out-of-loop signal (OOL) were performed. Upper bounds and approximate values of the in general frequency dependent transfer functions are given.

frequency noise. A compound actuator, the VCO at low frequencies and the error point injection at high frequencies, would combine both advantages. So far it has not been decided which control inputs will be used by the other subsystems to control the PSL frequency.

To verify that the feedback control loop is working as expected, we measured the in-loop residual frequency noise. No second reference cavity was available in our setup. Thus we were not able to measure the frequency noise in an independent out-of-loop measurement. However during Inital LIGO, with its very similar frequency stabilization, an out-of-loop measurement with the input mode-cleaner demonstrated a residual frequency noise level that was below the design requirements for Advanced LIGO. In order to deduce at least an upper bound for the frequency noise we used a DBB to measure the frequency noise out-of-loop downstream of the PMC. However the resonator and/or the frequency sensing of the DBB did not have the required noise performance to demonstrate the required stability.

#161737 - $15.00 USD Received 18 Jan 2012; revised 27 Feb 2012; accepted 4 Mar 2012; published 24 Apr 2012

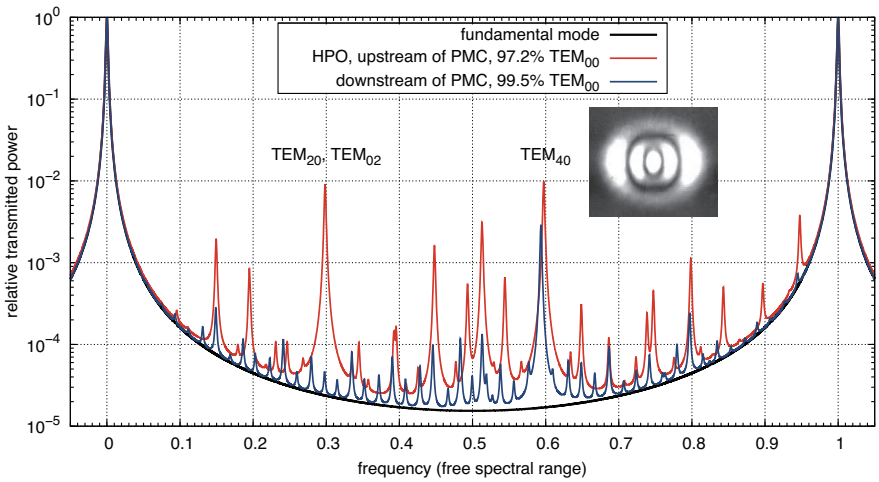

Fig. 4. Modescan performed with a DBB upstream and downstream of the PMC. The PMC suppressed higher order transverse modes and increased the power fraction in the TEM_{00} mode from 97.2% to 99.5%. A CCD image of the TEM_{40} in transmission of the PMC is shown.

2.4. Cross coupling

To characterize the interaction of the different feedback control loops we measured the transfer functions between various signals of the PMC locking, power stabilization, injection locking and frequency stabilization control loops. The transfer functions were measured in the frequency band from 10 Hz to 100 kHz using a network analyzer. The source signals were injected at the error points of the control loops since all control loops considered had bandwidths of at least several kilohertz. An overview of the cross coupling transfer functions measured is shown in Fig. 3.

3. Results

The PSL was running continuously for more than 18 months, interrupted only by short periods. The typical and maximum power downstream of the PMC were respectively 140 W and 150 W. The typical power was about 15% lower than the Advanced LIGO PSL goal of 165 W. We expect that the typical power of the observatory lasers will be slightly higher at around 150 W. A lower typical power of 150 W would slightly reduce the Advanced LIGO sensitivity in the shot noise limited frequency band to $(150\,\mathrm{W}/165\,\mathrm{W})^{1/2} = 0.95$ compared to the design goal.

In general the power was slowly decreasing, probably due to aging of the laser pump diodes of the HPO. However, this expected power degradation was compensated for on a regular interval by increasing the pump diode currents.

3.1. Beam quality

We measured a higher-order mode fraction of $2.8 \pm 0.1\,\%$ at the output of the HPO (see Fig. 4). The PMC efficiently reduces the higher-order mode fraction to only $0.50 \pm 0.01\,\%$ downstream of the PMC (see Fig. 4). Thus 99.5% of the power was in the TEM_{00} mode which was much better than the design requirement of $> 95\%$. The largest residual higher-order mode downstream of the PMC was the TEM_{40}, identified with a CCD camera, at about 0.6 FSR of the DBB resonator with a relative power of 0.003 (see Fig. 4). In the beam upstream of the PMC

#161737 - $15.00 USD Received 18 Jan 2012; revised 27 Feb 2012; accepted 4 Mar 2012; published 24 Apr 2012

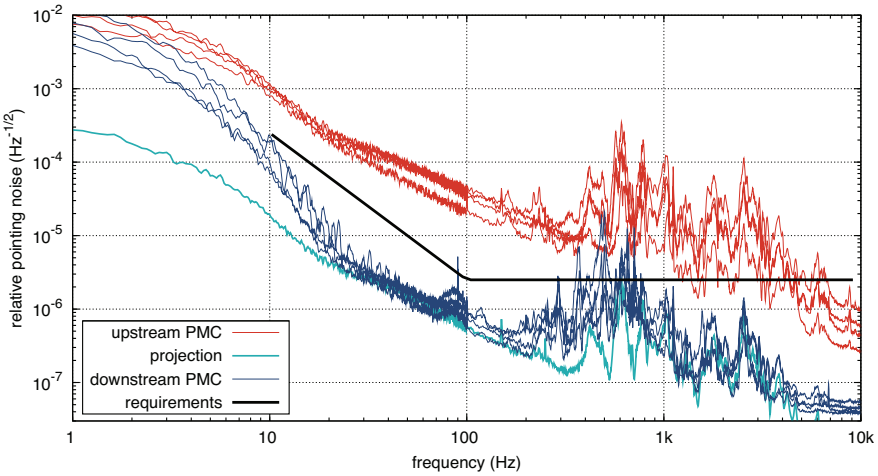

Fig. 5. Beam pointing fluctuations measured with a DBB upstream and downstream of the PMC. All four degrees of freedom, shift and tilt in horizontal and vertical directions, were measured at both locations. The PMC reduced the pointing fluctuations below the design requirements. For reference, one measurement upstream of the PMC was projected downstream of the PMC using the expected pointing suppression factor of the PMC.

this mode had a relative power of about 0.01. Without thermal effects in the PMC and its associated Gouy phase shift we expected that the PMC should suppress this mode by a factor of 1400. However, due to the thermal effects the resonance frequency of the TEM_{40} was close to one of the TEM_{00} modes and the suppression factor was reduced to 3.7 .

Based on the measurement of the LG_{10} and TEM_{40} power fraction as function of the transmitted power P we determined a power dependence of the eigenmode waist size of $w_0(P) = 555.53\,\mu\text{m} + 0.23\,\mu\text{m/W} \cdot P$ and of the round-trip Gouy phase of $\zeta(P) = 0.275\,\text{FSR} - 135 \times 10^{-6}\,\text{FSR/W} \cdot P$. At a transmitted power of 190 W the round-trip Gouy phase would be 0.25 FSR yielding no suppression of TEM modes of order $4 \cdot n$.

The power in reflection of the PMC dropped to 4.6% from the off-resonant to resonant PMC condition. This number was larger than the measured higher order mode fraction of 2.8% which might indicate a not perfectly impedance matched resonator or a slight offset in the PMC locking electronics causing an off-center stabilization to the resonance peak.

3.2. Beam pointing fluctuations

The beam pointing fluctuations downstream of the PMC decreased towards higher frequencies, with many peaks and resonances between 300 Hz and 7 kHz (Fig. 5). The differences between the four degrees of pointing freedom, shift and tilt in horizontal and vertical directions, were quite small. The measured level was below the PSL design requirements except for some peaks around 500 Hz. Since the beam pointing fluctuations depend strongly on the environment we expect that they will be fulfilled in the much quieter environment at the observatory sites in the whole frequency band. For comparison, the pointing fluctuations upstream of the PMC were measured as well (Fig. 5). This measurement verified the expected pointing suppression factor of 61 for the PMC since the measured pointing noise upstream of the PMC projected with this filter factor yielded almost the measured pointing noise downstream of the PMC. Discrepancies, especially at low frequencies, could be caused by moving components in the DBB or in the beam path to the DBB.

#161737 - $15.00 USD Received 18 Jan 2012; revised 27 Feb 2012; accepted 4 Mar 2012; published 24 Apr 2012

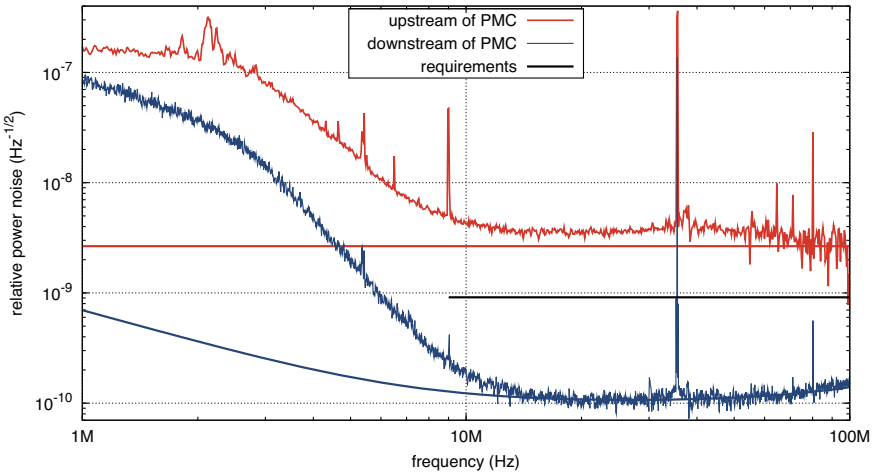

Fig. 6. Relative power noise at radio frequencies measured upstream and downstream of the PMC. The filtering of the PMC reduced the power noise below the design requirements. Both measurements were limited by shot noise (solid lines) for frequencies above about 10 MHz. The peak at 35.5 MHz is caused by phase modulation sidebands required for injection and PMC locking.

3.3. Relative power noise

We measured a relative power noise of $2 \times 10^{-7}\,\mathrm{Hz}^{-1/2}$ at 1 MHz upstream of the PMC, steeply rolling-off for frequencies above about 2 MHz (Fig. 6). The measurement was limited by shot noise at about $2 \times 10^{-9}\,\mathrm{Hz}^{-1/2}$ for frequencies above 9 MHz. The power noise downstream of the PMC was, as expected, filtered by the PMC with a low-pass corner frequency of 560 kHz. Using the optical ac coupling technique [25] we measured a power noise level of $10^{-10}\,\mathrm{Hz}^{-1/2}$ for frequencies above 10 MHz, where the measurement was limited by shot noise. The power noise was, as required, below $9 \times 10^{-10}\,\mathrm{Hz}^{-1/2}$ for frequencies above 9 MHz. Sharp peaks at 2 MHz, 5.5 MHz, 6.5 MHz, 9 MHz, 35.5 MHz, and 80 MHz were in the spectrum. The peak at 35.5 MHz was caused by the phase modulation used for the PDH sensing and the peak at 80 MHz by the driving frequency of the AOM power actuator. The origins of the other peaks were unknown and need further investigation.

The in-loop relative power noise of the first power stabilization loop was below the out-of-loop noise for frequencies below 2 kHz and was below the shot noise level for frequencies below 1 kHz (Fig. 7). The out-of-loop noise reached the lowest level of $2 \times 10^{-8}\,\mathrm{Hz}^{-1/2}$ between 60 Hz and 1 kHz, roughly corresponding to the calculated shot-noise level of $1.4 \times 10^{-8}\,\mathrm{Hz}^{-1/2}$. The out-of-loop noise increased towards lower frequencies up to about $10^{-6}\,\mathrm{Hz}^{-1/2}$. Line harmonics at 50 Hz, 100 Hz, 150 Hz, 200 Hz, 250 Hz were present in the spectrum. The power stabilization reduced the free running power noise (Fig. 7) by up to 3 orders of magnitude.

Peak-to-peak power fluctuations of the beam coupled into the PMC of about 11% over one hour were measured and were compensated by the control loop and the AOM. We observed that the peak-to-peak fluctuations depended strongly on the alignment of the beam to the PMC. Thus the low frequency peak-to-peak fluctuations seemed to be prone to be dominated by low-frequency pointing fluctuations in combination with small alignment offsets. Upstream of the PMC we measured peak-to-peak fluctuations of 5.5%. A comparison of the AOM diffraction signal noise which corresponds to the free running power noise of the beam coupled into the PMC and the free running power noise of the high-power oscillator showed only small discrep-

#161737 - $15.00 USD Received 18 Jan 2012; revised 27 Feb 2012; accepted 4 Mar 2012; published 24 Apr 2012

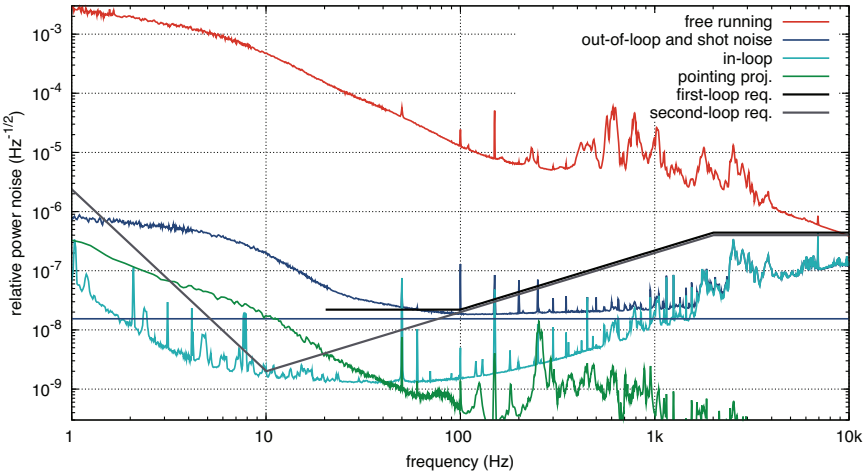

Fig. 7. Relative power noise in the detection band. The first power stabilization loop reduced the free running power fluctuations by several orders of magnitude. The out-of-loop measured power noise fulfills its requirements for frequencies above 60 Hz. The design requirements of the second loop are shown only for reference. A projection of the pointing noise showed that the out-of-loop measurement was not limited at low frequencies by this noise source.

ancies in the measurement frequency band from 1 Hz to 10 kHz. Thus beam pointing fluctuations at the PMC did not increase the power noise level significantly in this higher frequency band.

The origin of the noise in excess of shot-noise at frequencies below 60 Hz in the out-of-loop measurement was not clear. In particular a measurement made in the low-power mode of the laser system showed a better performance at these frequencies, achieving shot-noise limited performance down to 20 Hz.

With the QPD we measured transverse beam position fluctuations of about $4\,\mathrm{nm\,Hz^{-1/2}}$ at 10 Hz. For frequencies above 200 Hz many resonances and peaks were visible in the spectrum. We measured a coupling factor between pointing and out-of-loop relative power noise of $1.7\,\mathrm{m^{-1}}$ in the horizontal and of $4\,\mathrm{m^{-1}}$ in the vertical direction. A projection of the beam position fluctuations showed that the excess noise below 60 Hz cannot be explained by pointing (Fig. 7). The projection was more than one order of magnitude below the out-of-loop noise.

The out-of-loop power noise was below the first-loop-design-requirement for frequencies higher than 60 Hz. For reference the design requirements for the second-loop are shown (Fig. 7) which however must be achieved at a different location, at the input to the interferometer.

3.4. Frequency noise

Without frequency stabilization the frequency noise was roughly a factor of 3 above the typical NPRO frequency noise (Fig. 8). When activated, the frequency stabilization reduces the error point noise to more than one order of magnitude below the design requirements for the PSL (Fig. 8). This in-loop measurement showed that the control loop was working fine and had enough loop gain to reach the PSL design requirements. This was, however, an in-loop measurement and the actual frequency noise of the PSL as seen by the suspended mode-cleaner might be higher. The estimated shot noise level of the sensing was at $61\,\mu\mathrm{Hz\,Hz^{-1/2}}$ which was far below the measured in-loop frequency noise and was thus not a limiting noise source.

#161737 - $15.00 USD Received 18 Jan 2012; revised 27 Feb 2012; accepted 4 Mar 2012; published 24 Apr 2012

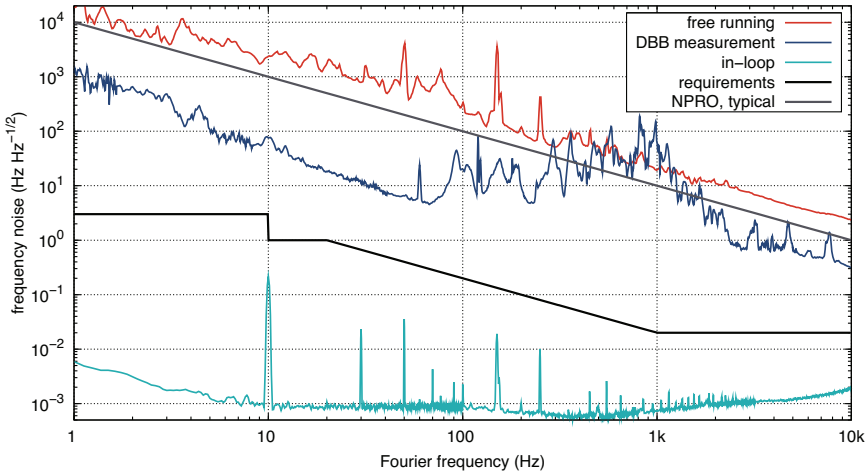

Fig. 8. Frequency noise measured downstream of the PMC with and without frequency stabilization. The measured in-loop frequency noise was consistent with the design requirements. To deduce an upper bound for the actual frequency noise an out-of-loop measurement with the DBB was performed with engaged frequency stabilization.

An out-of-loop measurement performed with the DBB showed a reduction of the free running frequency noise by up to two orders of magnitude. This measurement was an upper bound for the actual frequency noise of the PSL since it represents the combined noise of the DBB and the frequency noise. We believe that the measurement was dominated by the sensing noise of the DBB since due to its various purposes the resonator and the sensing of the DBB were not optimized for a frequency noise measurement.

3.5. Cross coupling

The transfer functions that were measured to determine the cross coupling between the control loops were in general quite noisy. Thus we were able to determine only upper bounds for the cross couplings (Fig. 3). Except for a few exceptions mentioned below the cross couplings were rather small or at the expected levels and caused no instabilities when all control loops were engaged.

We observed an unexpectedly high cross coupling between laser power modulation and the actuator signal of the frequency stabilization of $< 10^8\,\mathrm{Hz}/1$ (Fig. 3 d). This coupling might be critical and could limit the performance of the frequency stabilization. A projection of the out-of-loop measured power noise yielded a frequency noise level roughly at the frequency noise design requirements. As mentioned before the coupling measurements were quite noisy and thus this projection was only an upper bound. All other noise projections showed no coupling that would limit the noise performance of the power or frequency stabilization.

Furthermore the transfer function from frequency modulation to the injection locking control signal (Fig. 3 i) was much larger than expected. We measured a level of about $10^3\,\mathrm{Hz}/\mathrm{Hz}$ in contrast to the expected level of $1\,\mathrm{Hz}/\mathrm{Hz}$. We cannot explain the measured value other than stating that the measured value was only an upper bound and thus would be consistent with our expectations.

#161737 - $15.00 USD Received 18 Jan 2012; revised 27 Feb 2012; accepted 4 Mar 2012; published 24 Apr 2012

4. Conclusions

The Advanced LIGO PSL delivered an ultra-stable, high-power laser beam. Meeting the stringent design requirements of Advanced LIGO required elaborate active and passive stabilization schemes which reduced the laser noise by several orders of magnitude. With the comprehensive characterization of two PSLs, the reference system and the first observatory system, we were able to show that most design requirements for Advanced LIGO were fulfilled. Only the first-loop power stabilization at low frequencies showed excess noise not reaching its goal; this is not critical for the Advanced LIGO project, because the second power stabilization loop will be responsible for the ultimate power stability. The typical output power of 140 W of the reference system was about 15% lower than the goal of 165 W. However, the first observatory system had an output power of 157 W after installation. No long-term average value is available yet. Furthermore, although the in-loop measured frequency stability was consistent with the design requirements, an out-of-loop measurement would be necessary to state that the frequency noise design requirements were met. Such an out-of-loop measurement will be performed using the input mode-cleaner in the future. Since the frequency stabilization concept is very similar to Initial LIGO and key hardware components are reused, we expect to reach the same stability as in Initial LIGO which would fulfill the frequency noise requirements for Advanced LIGO.

The measurement and analysis of possible cross couplings between different control loops showed no critical coupling affecting control loop stability or noise performance. Some coupling factors were larger than expected and might need further investigation.

The computer system monitored the state of the PSL and performed fast and automatic lock acquisitions. Thus we were able to reliably and continuously operate the PSL in a 24h mode. Interruptions were necessary only due to a few failures caused by experiments during installation and optimization, due to power outages, or due to regular short maintenance intervals.

Many stabilization schemes employed in the PSL can be easily adapted to other continuous-wave single-frequency laser systems. Thus various other high-precision optical experiments can use these techniques to reduce laser noise which might limit their sensitivity.

The PSL is a crucial subsystem of Advanced LIGO, and most other subsystems rely on the PSL. Thus it plays an important role in the success of the Advanced LIGO detector which is expected to detect gravitational waves on a regular basis in the near future.

Acknowledgment

This research is supported by the Deutsche Forschungsgemeinschaft as a part of the QUEST cluster of excellence and the German Volkswagen Stiftung. LIGO was constructed by the California Institute of Technology and the Massachusetts Institute of Technology with funding from the National Science Foundation and operates under cooperative agreement PHY-0823459.

#161737 - $15.00 USD Received 18 Jan 2012; revised 27 Feb 2012; accepted 4 Mar 2012; published 24 Apr 2012